



Reconstruction of sound fields with a spherical microphone array

Efren Fernandez-Grande, Tim Walton

Acoustic Technology, Department of Electrical Engineering, DTU
Technical University of Denmark

ABSTRACT

Spherical microphone arrays are very well suited for sound field measurements in enclosures or interior spaces, and generally in acoustic environments where sound waves impinge on the array from multiple directions. Because of their directional properties, they make it possible to resolve sound waves traveling in any direction. In particular, rigid sphere microphone arrays are robust, and have the favorable property that the scattering introduced by the array can be compensated for - making the array virtually transparent. This study examines a recently proposed sound field reconstruction method based on a point source expansion, i.e. equivalent source method, using a rigid spherical array. The study examines the capability of the method to distinguish between sound waves arriving from different directions (i.e., as a sound field separation method). This is representative of the potential of the method to perform sound field identification and visualization in non-anechoic spaces, and ultimately for general in-situ measurements.

Keywords: Sound radiation, microphone arrays, spherical arrays, acoustic holography

I-INCE Classification of Subjects Number(s): 74.7, 23.1, 01.2

1. INTRODUCTION

Spherical microphone arrays are particularly convenient for measurements in interior spaces, enclosures, or in acoustic environments where sound waves arrive to the array from multiple directions [1–3], to a large extent because of their geometry (other common array configurations cannot distinguish between waves coming from different sides of the array, or the array properties depend on the direction of incidence of the waves [4]). In addition to this, rigid spherical microphone arrays are robust, and the scattering introduced by the array can be compensated for, making the array virtually transparent - which conveys great potential to the measurement principle.

This paper deals with the reconstruction of sound fields based on measurements with a rigid spherical microphone array, i.e. to capture a sound field at a measurement surface, to then ‘predict’ the entire sound field elsewhere, inferring the sound pressure, particle velocity and intensity vector, typically over a three-dimensional space. The approach differs from localization methods, in spite of the underlying similarities [5], in that the aim is *not only* to determine the direction from which waves arrive to the measurement area, but to estimate all acoustic quantities in any position in space based on the measured data.

Existing spherical holography methods rely on an expansion into spherical harmonics to provide a representation of the sound field. By means of ‘propagating’ the radial functions, they make it possible to predict either the total sound field [6, 7], or the incident sound field without the scattering introduced by the array [8–10]. Nevertheless, the domain of validity of existing methods is restricted to a spherical surface concentric to the array and entirely contained in the free-space (sources outside the domain). This imposes a limitation due to the obvious geometrical constraints. It is the motivation of the present work to address this matter.²

A method is proposed in this paper based on an equivalent source model [12] that takes into account the scattering introduced by the rigid spherical array. The entire sound field can be reconstructed at any point of the source-free domain without being restricted to a spherical surface, and the array’s scattering is compensated for. The study also examines the capability of the method to distinguish between sound waves arriving from different directions (i.e., as a sound field separation method), since this is representative of the potential of the method to perform sound field identification in non-anechoic spaces, and general in-situ measurements.

¹efg@elektro.dtu.dk

²An initial study was presented in a recent meeting [11]

2. THEORY

2.1 Background and existing methods

The existing methodologies for reconstructing sound fields using spherical arrays rely on expanding the measured sound field into a spherical harmonic expansion, to then make use of the radial functions (spherical Bessel) to reconstruct the sound field elsewhere. The most straightforward case is with an open spherical array; the reconstructed field is [13]

$$p(r, \Omega) = \sum_{n=0}^{\infty} \sum_{m=-n}^n \frac{j_n(kr)}{j_n(ka)} Y_n^m(\Omega) \int_{\Omega} p(a, \Omega) Y_n^m(\Omega)^* d\Omega, \quad (1)$$

where $p(a, \Omega)$ is the measured sound pressure. For notational simplicity the angular dependency is denoted by $\Omega \equiv (\theta, \phi)$ thus $\mathbf{r} = (r, \theta, \phi) \equiv (r, \Omega)$, and $d\Omega \equiv \sin\theta d\theta d\phi$, so that the integration over the sphere is $\int_{\Omega} (\cdot) d\Omega \equiv \int_0^{2\pi} \int_0^{\pi} (\cdot) \sin\theta d\theta d\phi$. The radius of the sphere is a , j_n is the spherical Bessel function of order n , k is the wavenumber, and $(\cdot)^*$ is the complex conjugate. The time dependency $e^{j\omega t}$ has been omitted, and the spherical Hankel functions are of the second kind, defined as $h_n^{(2)}(x) = j_n(x) - jy_n(x)$, where $y_n(x)$ is a spherical Neumann function of order n . From here onwards, $h_n^{(2)} \equiv h_n$. The Spherical harmonics $Y_n^m(\Omega)$ are defined as

$$Y_n^m(\theta, \phi) \equiv \sqrt{\frac{(2n+1)(n-m)!}{4\pi(n+m)!}} P_n^m(\cos(\theta)) e^{-jm\phi}. \quad (2)$$

Consider a microphone array flush-mounted on a rigid sphere. The total sound field is naturally composed of the incident and the scattered sound, and it can be expanded into spherical harmonics as [7]

$$p_t(r, \Omega) = \sum_{n=0}^{\infty} \sum_{m=-n}^n (ka)^2 [j_n(kr)y_n'(ka) - j_n'(ka)y_n(kr)] Y_n^m(\Omega) \int_{\Omega} p(a, \Omega) Y_n^m(\Omega)^* d\Omega. \quad (3)$$

Equation (3) makes it possible to reconstruct the *total* sound field, incident plus scattered, in free-space at any other radius than measured. This expression is the one used in Ref. [7].

Nevertheless, it is also possible to compensate for the scattering introduced by the rigid sphere array. The principle is to reconstruct the sound field, based on only the basis functions that describe the incident sound field. The incident pressure can be reconstructed as [9]

$$p_i(r, \Omega) = j(ka)^2 \sum_{n=0}^{\infty} \sum_{m=-n}^n h_n'(ka) j_n(kr) Y_n^m(\Omega) \int_{\Omega} p(a, \Omega) Y_n^m(\Omega)^* d\Omega. \quad (4)$$

This is the expression given in Ref. [9], although here it has been simplified via the Wronksian relationship.

It is apparent from Eqs. (3) and (4) that the reconstruction in all three cases is based upon the propagation of the radial functions $j_n(kr)$ and $y_n(kr)$ from the measurement radius (a) to a different one (r). However, this expansion - being a solution to the Helmholtz equation, is only valid for the source-free medium, i.e., between the radius of the sphere $r = a$ and the closest source or boundary $r = r'$. This imposes a limitation due to geometrical constraints, and it is not possible to reconstruct the sound field very close to a source or boundary, unless it is approximately spherical, an unlikely general case. The proposed method overcomes this limitation.

2.2 Sound field due to a point source

Let there be a point source at $\mathbf{r}_0 = (r_0, \theta_0, \phi_0)$ with volume velocity Q , radiating in the presence of a rigid sphere centered at the origin of coordinates. The total sound pressure is a sum of the incident waves and the waves scattered by the sphere, $p_t(r, \Omega) = p_i(r, \Omega) + p_s(r, \Omega)$. The incident sound pressure is

$$p_i = \frac{j\omega\rho Q e^{-jkR}}{4\pi R} = j\omega\rho Q G(\mathbf{r}, \mathbf{r}_0), \quad (5)$$

where $G(\mathbf{r}, \mathbf{r}_0)$ is the free-field Green's function and $R = |\mathbf{r}_0 - \mathbf{r}|$ is the distance between the observation point and the position of the point source. In a spherical harmonic expansion, the incident pressure p_i takes the general form of a so-called 'complete solution'

$$p_i(\mathbf{r}) = \sum_{n=0}^{\infty} \sum_{m=-n}^n A_{mn} j_n(kr) h_n^{(2)}(kr_0) Y_n^m(\Omega) Y_n^m(\Omega_0)^*, \quad (6)$$

and the free-space Green's function in spherical harmonics is [7]

$$G(\mathbf{r}, \mathbf{r}_0) = -jk \sum_{n=0}^{\infty} \sum_{m=-n}^n j_n(kr) h_n(kr_0) Y_n^m(\Omega) Y_n^m(\Omega_0)^*. \quad (7)$$

From which the A_{mn} coefficients are obtained as $A_{mn} = \rho ck^2 Q$. On the other hand, the scattered pressure p_s takes the form of a 'radiation solution'

$$p_s(\mathbf{r}) = \sum_{n=0}^{\infty} \sum_{m=-n}^n B_{nm} h_n(kr) Y_n^m(\Omega). \quad (8)$$

The boundary condition of the problem dictates that the radial component of the particle velocity must vanish at the boundary ($r = a$), the surface of the rigid sphere, $\frac{\partial p_i}{\partial r} \Big|_{r=a} + \frac{\partial p_s}{\partial r} \Big|_{r=a} = 0$, from which the scattering coefficients can be calculated, $B_{mn} = -A_{mn} \frac{j_n(ka)}{h_n^{(2)}(ka)} h_n(kr_0) Y_n^m(\Omega_0)^*$, yielding the total sound pressure

$$p_t(\mathbf{r}) = \rho ck^2 Q \sum_{n=0}^{\infty} \sum_{m=-n}^n \left(j_n(kr) - \frac{j_n(ka)}{h_n^{(2)}(ka)} h_n(kr) \right) h_n(kr_0) Y_n^m(\Omega) Y_n^m(\Omega_0)^*. \quad (9)$$

Finally making use of the Wronskian relation, the pressure on the surface of the sphere at (a, Ω) , due to a point source in (r_0, Ω_0) is simplified to

$$p_t(a, \Omega) = \frac{-j\rho c Q}{a^2} \sum_{n=0}^{\infty} \sum_{m=-n}^n \frac{h_n^{(2)}(kr_0)}{h_n^{(2)}(ka)} Y_n^m(\Omega) Y_n^m(\Omega_0)^*. \quad (10)$$

From the addition theorem, this expression can be simplified further, due to the rotational axisymmetry of the field around the axis from the center of the sphere to the point source, yielding it only as a function of the Legendre polynomials, with constant azimuth, instead of the full spherical harmonic solution. Nonetheless the latter general case, Eq. (10), is considered here.

2.3 Method: Point source expansion with a rigid spherical array

The essential idea behind the proposed method is to use Eq. (10) as the basis to describe an arbitrary sound field as a superposition of the waves radiated by a combination of point sources that are placed outside the domain of interest. This domain can be of arbitrary shape, as opposed to existing methods. The equivalent sources can be placed either inside a source under study (for instance a radiation problem, where the source is 'substituted' by a combination of point sources), or outside the domain inside which the sound field is reconstructed (if for instance one is concerned with reconstructing the sound field over a certain volume in a free-field, or inside an enclosure, etc.).

The pressure on the surface of the sphere at (a, Ω_k) , due to a point source in (r_0, Ω_0) is the one given in Eq. (10). Based on this, the sound pressure measured on each of the K transducers of the array can be expanded as a continuous distribution of point sources over a surface S . This surface is where the point sources are placed, thus S is associated with $\mathbf{r}_0 = (r_0, \Omega_0)$

$$p_t(a, \Omega_k) = \iint_S \frac{-j\rho c Q(\mathbf{r}_0)}{a^2} \sum_{n=0}^{\infty} \sum_{m=-n}^n \frac{h_n^{(2)}(kr_0)}{h_n^{(2)}(ka)} Y_n^m(\Omega_k) Y_n^m(\Omega_0)^* dS, \quad (11)$$

or, using a discrete distribution of L equivalent sources,

$$p_t(a, \Omega_k) = \sum_{l=1}^L \frac{-j\rho c Q_l}{a^2} \sum_{n=0}^{\infty} \sum_{m=-n}^n \frac{h_n^{(2)}(kr_{0,l})}{h_n^{(2)}(ka)} Y_n^m(\Omega_k) Y_n^m(\Omega_{0,l})^*. \quad (12)$$

Conducting the summation over the angle and radial functions (over m and n), in practice truncated at $\sum_{n=0}^N \sum_{m=-n}^n$ (see Sect. 3), it is possible to express the total sound pressure p_t at a discrete set of K points on the sphere, in matrix form as

$$\mathbf{p}_t = \mathbf{G}_N \mathbf{q}, \quad (13)$$

where \mathbf{p}_t is a $K \times 1$ vector with the measured pressures, \mathbf{q} a $L \times 1$ vector with the yet unknown source strengths (note that they are $j\omega\rho Q_l$), and \mathbf{G}_N a $K \times L$ transfer matrix between the source strengths and the total measured

pressures on the sphere. This is typically an underdetermined problem, ill-posed when r is between the source and the array, requiring regularization for it's inversion [10, 14],

$$\mathbf{q} = \mathbf{G}_N^{-1} \mathbf{p} = \mathbf{V} \mathbf{F} \mathbf{\Sigma}^{-1} \mathbf{U}^H \mathbf{p}. \quad (14)$$

The regularized inversion (\mathbf{G}_N^{-1}) is performed based on a singular value decomposition of $\mathbf{G}_N = \mathbf{U} \mathbf{\Sigma} \mathbf{V}^H$, where \mathbf{U} and \mathbf{V}^H are unitary vectors and $\mathbf{\Sigma}$ contains the singular values of the transfer matrix. The matrix \mathbf{F} is a diagonal matrix that contains the regularization filter factors, in this study either truncated at σ_{max} or using Tikhonov regularization $F_{ii} = \sigma_i^2 / (\sigma_i^2 + \lambda^2)$, with λ the regularization parameter. This parameter will determine the ‘weight’ of the singular values in the solution, so that the noisy terms are left out of the reconstruction.³

Once the strength of the sources has been determined, the incident sound pressure can be predicted anywhere in the domain of interest

$$\mathbf{p}_i = \mathbf{G} \mathbf{q}, \quad (15)$$

where \mathbf{G} is a reconstruction matrix that consists of the Green's function in free-space between the position of the sources \mathbf{r}_0 and the reconstruction points, as in Eq. (5). This fact signifies that the scattering introduced by the sphere is not present in the reconstructed field, since it is based on the free-field sound pressure radiated by each point source. The total pressure could be reconstructed using \mathbf{G}_N instead.

The particle velocity vector can be calculated from Euler's equation of motion, $\mathbf{u} = \frac{-1}{j\omega\rho} \nabla p$, or introducing the gradient of the Green's function $\mathbf{G}_\nabla = \nabla G(\mathbf{r}, \mathbf{r}_0)$

$$\mathbf{u} = \frac{-1}{j\omega\rho} \mathbf{G}_\nabla \mathbf{q}, \quad (16)$$

and correspondingly the sound intensity vector as

$$\mathbf{I} = \frac{1}{2} \text{Re}\{p \mathbf{u}^*\}, \quad (17)$$

where $(\cdot)^*$ is the complex conjugate. It is apparent from these equations that the reconstruction provides a complete characterization of the acoustic field. This method can be understood as an extension of the equivalent source method or wave superposition method to measurements with a rigid sphere microphone array. It can be used to reconstruct over arbitrary geometries, and the scattering introduced by the array is compensated for.

3. NUMERICAL RESULTS

A numerical study is conducted to test the proposed method, compare it to the existing ones and examine its accuracy. In the simulated measurements, the array used is a rigid sphere array of radius 9.75 cm, with 50 microphones, distributed nearly uniformly, and with a sampling that limits the expansion to $N \leq 5$ orders (so that the orthogonality of the spherical wave expansion is satisfied [9]), and also provided that $N > ka$ to prevent spatial aliasing. In the following, the error is calculated as

$$E[\%] = \|\mathbf{p}_{true} - \mathbf{p}_i\|_2 / \|\mathbf{p}_{true}\|_2 \quad (18)$$

3.1 Comparison with previous methods

In this section, the proposed method is compared to a previously existing method, spherical near-field acoustic holography (SNAH), as described by Eq. (4) [9]. The source used is a monopole 40 cm away from the center of the array, with volume velocity of $10^{-5} \text{ m}^3/\text{s}$. The equivalent sources consist of a grid of 20×20 sources over a $10 \times 10 \text{ cm}^2$ plane 41 cm away from the center of the array. Additive noise of 30 dB signal-to-noise ratio relative to the measured pressure was added to the simulated measurements. In both cases, the regularization used is truncated singular value decomposition [10] via the filter factors as described in section 2.3. The reconstruction positions are shown in Fig. 1, a line from the monopole passing through the center of the array.

Figure 2 shows the results from the reconstruction. It is clear how the proposed method (here denoted Spherical-ESM) is much more accurate, particularly far from the array, and also away from the source. The reason for this is that in the reconstruction with SNAH Eq. (4), the ill-conditioning is due to the amplification introduced by the radial functions for $r > a$, in all angular directions. Contrarily, the proposed Spherical-ESM method is only ill-conditioned when the reconstruction takes place between the array and the equivalent sources (which entails a back-propagation of the waves towards the source). In the general case, the equivalent source method is more suitable for modeling radiation problems.

³In the present study, except in Sect. 3.1, generalized cross validation (GCV) is used for choosing the regularization parameter and Tikhonov regularization to invert the problem.

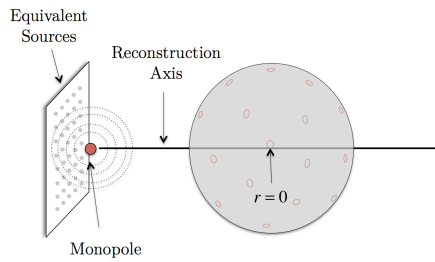


Figure 1 – Diagram showing the set up for spherical NAH and spherical ESM comparison

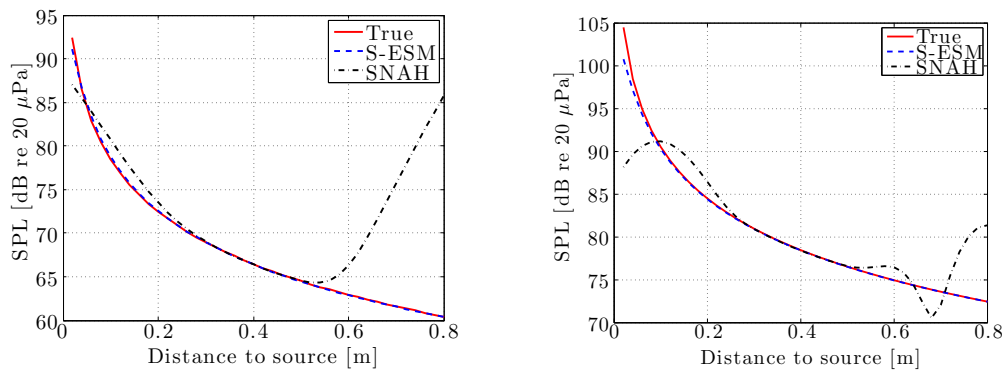


Figure 2 – Comparison of existing methods. Solid line - true pressure; dashed blue line - the proposed Spherical-ESM; Dash-dotted line - Spherical NAH. Left: $ka=0.5$. Right: $ka=2$

3.2 Sound field separation

This section examines the capability of the proposed method to distinguish between waves traveling in different directions. In this case, two monopole sources are considered, one regarded as the primary source, fixed at a certain position in front of the array, and a secondary source that is moved about and its level changed. Regarding how to model the sound field, two options are illustrated in Fig. 3: An option where there are two sets of equivalent sources, one for the primary source and another for the secondary source (Fig. 3a). The other option (Fig. 3b) is to distribute equivalent sources all around the array, with a denser mesh of sources to model the primary source. In general, the former option proved to be somewhat more accurate, but it requires that the position of the secondary source is approximately known.

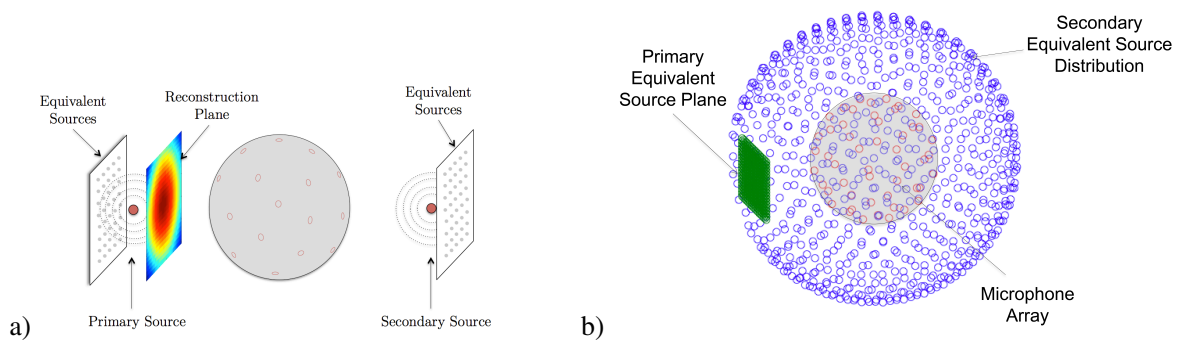


Figure 3 – Diagram showing two possible distributions of equivalent sources for sound field separation.

Figure 4 shows the error of the reconstruction as a function of the sound pressure radiated by the primary source relative to the sound pressure of the secondary source, in the following denoted as the primary-to-secondary source ratio,

$$PSR = 20\log(|p_{s1}/p_{s2}|) |_{r=0}, \tag{19}$$

p_{s1} is the sound pressure due to the primary source in a plane conformal to the equivalent sources that intersects the origin of coordinates $z = 0$ (center of the array) and p_{s2} is the sound pressure due to the secondary source at the same position. The two sources are placed 11 cm away from the surface of the array, and the equivalent sources are retracted 1 cm, they are distributed as in Fig. 4b, for the primary source as in the previous section,

and for the secondary source they are 350 equivalent sources distributed over a spherical surface of 21 cm radius. In this case the reconstruction takes place in the origin of coordinates (center of the array). Several other points were tested (in front and behind the array) that yielded very similar results. Figure 4 (left) shows

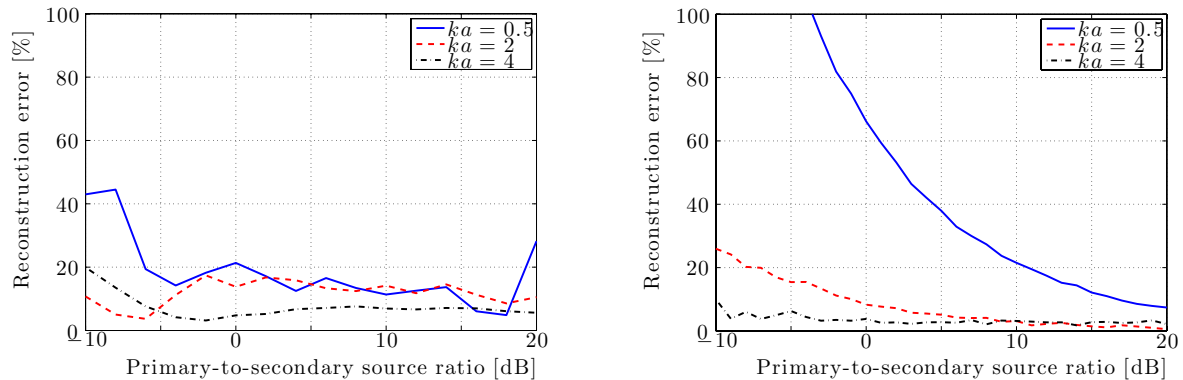


Figure 4 – Separation as a function of primary-to-secondary source ratio. Left: sound field separation with equivalent sources as in Fig. 3b. Right: without sound field separation, modeling only the contribution of the primary source. Reconstruction at the $z = 0$ plane

the reconstruction error as a function of the primary-to-secondary source ratio, the ‘true’ pressure being the one radiated by the primary source; Figure 4 (right) also shows the reconstruction error, but in this case, the sound field is not separated; only the equivalent sources for the primary source are used. In this case, the error is much greater, especially at low frequencies, and less critical at high frequencies. The results indicate that if the disturbance from the secondary source is weak, the separation is not required. However, when the contribution of the secondary source is comparable to the primary one, the separation proves more accurate.

Figure 5 shows the separation accuracy as a function of the relative angle between the position of the sources, where 180° corresponds to the secondary source at the opposite side of the array as in Fig 3a, and 0° to the sources in the same position. As expected, the error is fairly independent of the angle.

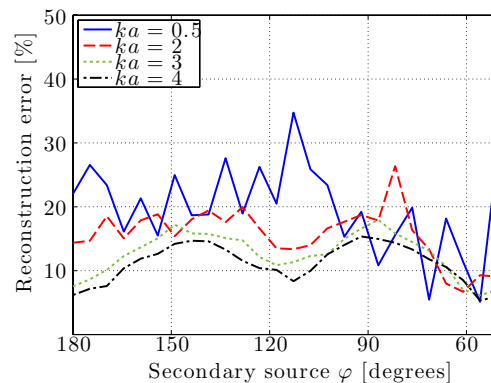


Figure 5 – Reconstruction accuracy using an equivalent source mesh as in Fig 3b, as a function of angle. The secondary source is radiating as much as the primary source. Reconstruction at plane $z = 0$.

4. EXPERIMENTAL RESULTS

This section presents results from measurements (see Fig. 6), in the anechoic chamber at DTU (1000 m^3), with a B&K spherical array of 50 1/4' microphones, of radius 9.75 cm, using two B&K Omnisource loudspeakers that radiate approximately like a point source, driven with white noise. The primary source and the spherical array were fixed, and the secondary source could be moved around the array and its output level varied. The primary and secondary source were placed 23 cm and 56 cm away from the surface of the array respectively. The equivalent sources were placed as in Fig. 3a, with two planes of 20×20 equivalent sources 24 cm away from the array surface, covering an area of $10 \times 10 \text{ cm}^2$. The measured data was captured in Pulse and post-processed in Matlab. A uniform 60 channel planar array was used as to measure the ‘true’ pressure. However, this ‘true’ sound pressure is far from ideal, since the microphones have different responses, there is electrical noise, positioning errors, and the array introduces diffraction and scattering. All these factors contribute to ‘artificially’ increasing the estimated errors in the experimental results.

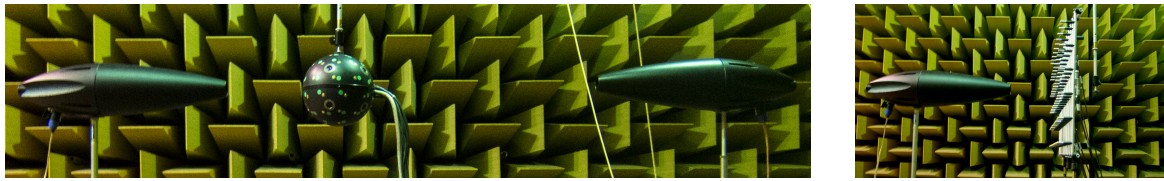


Figure 6 – Pictures of the measurements with the spherical array in the presence of primary and secondary source (left) and the primary source with the reference planar array used to measure the ‘true’ pressure (right).

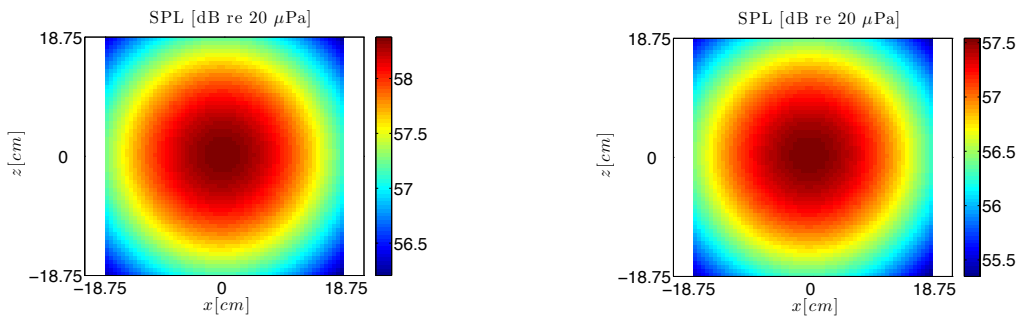


Figure 7 – Experimental results. Reconstructed sound pressure 20 cm in front of the array of primary source without secondary source, error 10% (left); reconstructed sound pressure of the primary source when the secondary source is radiating at the same level from the opposite side, error 18% - Equivalent sources as in Fig. 3a, $ka = 0.5$

Figure 7 (left) shows the magnitude of the reconstructed sound pressure 20 cm in front of the array (10 cm away from the loudspeaker) when only the primary source is radiating sound ($ka = 0.5$). The reconstruction error in this case is of approximately 10 %. Figure 7 (right) shows the reconstructed sound pressure where the secondary source is radiating as much as the primary one (primary-to-secondary source ratio of 0 dB) from the opposite side. Although the error in this case is slightly higher, 18 %, the overall reconstruction is acceptable and the pressure radiated by the first source is recovered satisfactorily.

Figure 8 (left) shows the error as a function of the primary-to-secondary source ratio (Eq. 19), and the angle where the secondary source is positioned (right). The reconstruction errors are significant, but in any case lower than 27 % (when interpreting the results, it should be considered that the uncertainty in the error estimation is comparable to the error of the method itself, setting a lower bound). In Fig. 8 (right) it can be seen that the error does not change when the secondary source is at different angles, a result that is expected.

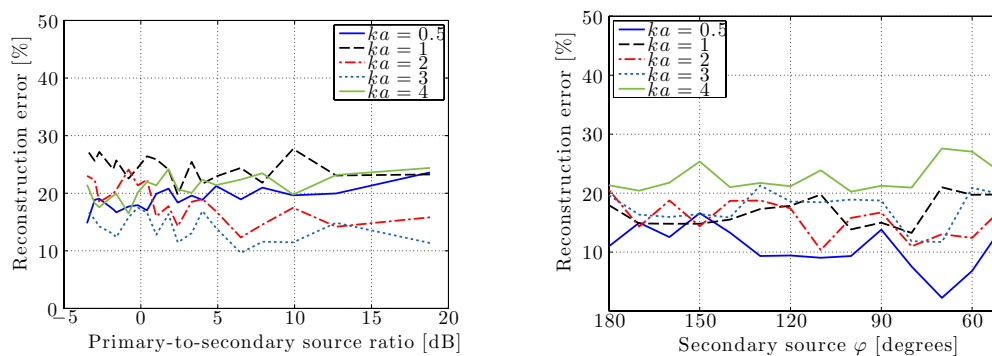


Figure 8 – Experimental results. Error as a function of primary-to-secondary level ratio and relative angle between the sources

5. CONCLUSIONS

This paper proposes a sound field reconstruction method based on measurements with a rigid spherical array. The method consists of an equivalent source expansion that takes into account the scattering introduced by the spherical array, and which makes it possible to reconstruct the sound field over any arbitrary geometry (in the present study just over a planar surface, although it could be any other geometry, separable or not). The scattering introduced by the sphere can be compensated for, consequently reconstructing only the incident

sound field, as if the array was not present.

The study shows that the method is more accurate than existing methods based on spherical harmonic expansions, partly because it is much more suited to radiation problems than a truncated expansion. Regarding the placement of the equivalent sources it is important to either make use of a-priori knowledge of the sound field, or choose an equivalent source distribution that can model the general case. The method makes it possible to distinguish between waves traveling in different directions, as demonstrated by the numerical and experimental results. These results are nearly independent on the angle of incidence of the incoming waves, and consistent for different relative levels between the waves (of about 15-20 dB). The reconstruction principle can be further applied to, for instance, absorption coefficient or impedance measurements; the results from the present study are encouraging.

ACKNOWLEDGEMENTS

The authors would like to thank Karim Haddad and Jørgen Hald at B&K for lending us the spherical array for the experimental measurements. This work was supported by the Danish Council for Independent Research DFF-FTP, under the grant # FTP/0602-02340B.

REFERENCES

1. B. Rafaely. Plane-wave decomposition of the sound field on a sphere by spherical convolution. *J. Acoust. Soc. Am.*, 116(4):2149–2157, 2004.
2. M. Park and B. Rafaely. Sound-field analysis by plane-wave decomposition using spherical microphone array. *J. Acoust. Soc. Am.*, 118(5): 3094–3103, 2005.
3. K. Haddad and J. Hald. 3d localization of acoustic sources with a spherical array. *Acoustics '08 Paris. Vol 123*, 123(5): 3311–3311, 2008.
4. E. Fernandez-Grande, F. Jacobsen, and Q. Leclere. Sound field separation with sound pressure and particle velocity measurements. *J. Acoust. Soc. Am.*, 132(6):3818–3825, 2012.
5. A. Pereira and Q. Leclere. Improving the equivalent source method for noise source identification in enclosed spaces. *Proceedings of ICSV 18, Rio de Janeiro, Brazil, 10-14 July, 2011*.
6. E. G. Williams and K. Takashima. Vector intensity reconstructions in a volume surrounding a rigid spherical measurement array. In *Acoustics '08 Paris. Vol 123*, page 3309, 2008.
7. E. G. Williams and K. Takashima. Vector intensity reconstructions in a volume surrounding a rigid spherical microphone array. *J. Acoust. Soc. Am.*, 127(2): 773–783, 2010.
8. F. Jacobsen, J. Hald, E. Fernandez-Grande, and G. Moreno. Spherical near field acoustic holography with microphones on a rigid sphere. In *Acoustics '08 Paris. Vol 123*, pp. 3385, 2008.
9. F. Jacobsen, G. Moreno-Pescador, E. Fernandez-Grande, and J. Hald. Near field acoustic holography with microphones on a rigid sphere. *J. Acoust. Soc. Am.*, 129(6):3461–3464, 2011.
10. A. Granados, F. Jacobsen, and E. Fernandez-Grande. Regularised reconstruction of sound fields with a spherical microphone array. *Proceedings of Meetings on Acoustics*, 19(1), 2013.
11. E. Fernandez-Grande. Reconstruction of arbitrary sound fields with a rigid-sphere microphone array. *166th Acoust. Soc. Am. meeting San Francisco, 2-6th December*, 134(5): 3998–3998, 2013.
12. G. H. Koopmann, L. Song, and J. B. Fahline. A method for computing acoustic fields based on the principle of wave superposition. *J. Acoust. Soc. Am.*, 86(6): 2433–2438, 1989.
13. E. G. Williams, N. Valdivia, and P. C. Herdic. Volumetric acoustic vector intensity imager. *J. Acoust. Soc. Am.*, 120(4): 1887–1897, 2006.
14. P. C. Hansen. *Rank-Deficient and Discrete Ill-Posed Problems: Numerical Aspects of Linear Inversion*. SIAM monographs on mathematical modeling and computation. SIAM, 1998.